



Selective removal of bromide and iodide from natural waters using a novel AgCl-SPAC composite at environmentally relevant conditions

Mohamed Ateia^a, Cagri Utku Erdem^a, Mahmut Selim Ersan^{a,b}, Marcel Ceccato^{c,d},
Tanju Karanfil^{a,*}

^a Department of Environmental Engineering and Earth Science, Clemson University, SC, 29634, USA

^b Water Quality Research and Development Division, Southern Nevada Water Authority, P.O. Box 99954, Las Vegas, NV, 89193-9954, USA

^c Carbon Dioxide Activation Center (CADIAC) - Interdisciplinary Nanoscience Center (iNANO), Aarhus University, Gustav Wiedes Vej 14, 8000, Aarhus C, Denmark

^d Department of Chemistry, Aarhus University, Langelandsgade 140, 8000, Aarhus C, Denmark

ARTICLE INFO

Article history:

Received 16 December 2018

Received in revised form

6 March 2019

Accepted 15 March 2019

Available online 20 March 2019

Keywords:

Superfine activated carbon

Silver chloride

Bromide

Iodide

Disinfection by-products

Water toxicity

ABSTRACT

The removal of bromide (Br^-) and iodide (I^-) from source waters mitigates the formation of brominated and iodinated disinfection by-products (DBPs), which are more toxic than their chlorinated analogues. In this study, we report on our recently developed environmental-friendly method for the preparation of novel silver chloride/superfine activated carbon composite (AgCl-SPAC) to rapidly and selectively remove Br^- and I^- from surface waters. The material characteristics were tracked, before and after treatment, using scanning electron microscopy (SEM), energy-dispersive X-ray (EDX), X-ray diffraction (XRD), and X-ray photoelectron spectra (XPS) spectroscopies. The results showed very fast removal kinetics of Br^- and I^- by AgCl-SPAC with equilibrium times at 150 s and <10 s, respectively (i.e., 2–3 orders of magnitudes faster than previously tested Ag-based composites). In addition, AgCl-SPAC was evaluated under eight different Cl^- concentrations up to 400 mg/L and exhibited high removal efficiencies for I^- (i.e., >90% at all tested conditions) and Br^- (i.e., >80% at $\text{Cl}^- = 0.5\text{--}200$ mg/L, and 60–75% at extreme Cl^- conditions = 300–400 mg/L). Unlike previous Ag-based composites, AgCl-SPAC performance was not affected by elevated concentrations of two types of natural organic matter (2–16 mg-NOM/L). The superior performance was further confirmed in four different surface waters and one groundwater. After the removal of Br^- and I^- from all waters by AgCl-SPAC, the subsequent DBPs formation (trihalomethanes, haloacetic acids, and haloacetonitriles), total organic halogens (TOX), bromine substitution factor (BSF), and calculated cytotoxicity under the uniform formation conditions (UFC) decreased significantly. Overall, this novel composite represents a promising alternative approach, to be integrated continuously or seasonally, for controlling the formation of brominated and/or iodinated DBPs at water treatment plants.

© 2019 Published by Elsevier Ltd.

1. Introduction

Bromide (Br^-) is ubiquitous in natural waters (e.g., rivers, groundwaters) with a concentration range of 100–3000 $\mu\text{g/L}$ (Amy et al., 1993; Weinberg et al., 2002), with elevated concentrations in waters affected by wastewater discharges and/or waters from hydraulic fracturing operations. Although Br^- itself is not toxic, it reacts with natural organic matter and disinfectants during water

treatment, which forms regulated disinfection byproducts (DBPs) such as bromate and brominated trihalomethane (THM) and haloacetic acid (HAA) (Richardson, 2014). Iodide (I^-) may also be present along with Br^- , with a reported average $\text{Br}^-:\text{I}^-$ mass ratio of approximately 10:1 in natural waters (Jones et al., 2012). During chloramination, I^- can result in the formation of highly toxic iodinated DBPs (Jones et al., 2011; Liu et al., 2018). The cyto- and genotoxicity results showed that the toxicity index of iodinated and brominated DBPs are $>10^5$ and $>10^4$ times their chlorinated analogues (i.e., regulated DBPs), respectively (Plewa et al., 2017). Thus, because they serve as the precursors of toxic DBPs, the removal of Br^- and I^- is essential for public health and regulatory compliance

* Corresponding author.

E-mail address: tkaranf@clemson.edu (T. Karanfil).

benefits. Meanwhile, the conventional water treatment technologies (coagulation/flocculation, activated carbon, etc.) are not effective in the removal of ambient Br^- and I^- (Richardson et al., 2007). Some advanced techniques, such as reverse osmosis, nanofiltration, electrolysis, and capacitive deionization showed a high removal of Br^- and I^- (Watson et al., 2012). However, membranes are expensive and may not be easily integrated into existing water treatment plants, and electrochemical removal of bromide involves oxidizing bromide to bromine that forms different toxic brominated DBPs (Dorji et al., 2018; Kimbrough and Suffet, 2002).

Previous studies have discussed the use of silver (Ag)-based techniques to remove Br^- and I^- from water by forming and precipitating the insoluble silver halogenides (i.e., silver bromide [AgBr] and silver iodide [AgI]). Three main application methods of silver for halide removal have been described in the literature. First, silver cathodes were used in electrolysis cells for the removal of Br^- (Bo, 2008). Second, silver-impregnated adsorbents were synthesized and tested for halide removal, such as Ag-impregnated carbon aerogels (Sanchez-Polo et al., 2007), activated carbons (Chen et al., 2017; Ho and Kraus, 1981; Hoskins et al., 2002), graphene oxides (Kidd et al., 2018), calcium alginate (Zhang et al., 2011), and polymers (Gong et al., 2013; Polo et al., 2016). Third, recent studies have demonstrated the direct use of silver salts (i.e., silver nitrate [AgNO₃]) (Gan et al., 2018) or silver nanoparticles (Polo et al., 2017) for the removal of halides from surface waters. However, several critical limitations have also been observed; including 1) the removal efficiency decreased when these materials were tested under typical water treatment conditions because of the competition with coexisting chloride ions (Cl^-) and natural organic matter (NOM), 2) the removal efficiency depended on the dispersion and the availability of silver solids on the sorbent surface, 3) all reported impregnation methods involved the oxidation of carbon surfaces which is not an environmentally friendly approach and results in hazardous concentrated acid wastes, 4) the impregnation methods utilized high silver nitrate concentration (50,000–75,000 mg/L), however, the silver content after the impregnation was still very limited, and 5) the direct use of silver (salts or particles) possess a high risk of silver release in the treated water. Therefore, new effective methods for halide removal are needed to address and overcome those limitations.

Herein, we report on our recently developed silver chloride on superfine activated carbon composite (AgCl-SPAC) for rapid and selective removal of Br^- and I^- from surface waters. We hypothesized that using AgCl will overcome the competition of Cl^- (which normally coexist in natural waters with Cl^- : Br^- ratio of 100–200). Besides, SPAC provides an extra advantage of fast removal kinetics and protects AgCl from photo-oxidation to maintain its high performance. The specific objectives were: i) synthesis and characterization of AgCl-SPAC composite, ii) test the composite performance under challenging conditions by elevating the concentration of Cl^- and different NOM, and iii) test the removal of Br^- and I^- from different surface waters and evaluate the subsequent change in the formation of DBPs.

2. Materials and methods

2.1. Activated carbons, chemicals and reagents

Three different granular activated carbons (GAC) (Filtrisorb 400 [bituminous coal, Calgon], Hydrodarco 3000 [lignite coal, Norit], and Aquacarb 1230C [coconut shell, Siemens]) were used to prepare SPAC with a bead mill (MiniCer, Netzsch Premier Technologies, Exton, PA, USA) as described in our previous study (Partlan et al., 2016). The selected physicochemical properties of the SPAC are summarized in Table 1. The Br^- , I^- and Cl^- stock solutions (1000 mg/L) were prepared by dissolving reagent grade (99.0%) sodium bromide (NaBr), sodium iodide (NaI), and sodium chloride (NaCl) salts (Sigma-Aldrich) in distilled-deionized water (DDW), and the desired concentrations were obtained by diluting the stock solutions with DDW.

2.2. Preparation and characterization of AgCl-SPAC composite

AgCl-SPAC composites were prepared by dissolving 1 g of AgNO₃ in 100 mL of ethanol (Sigma-Aldrich) before adding 1 g SPAC (all SPAC are stored in slurry form) and the mixture was placed on a magnetic stirrer for 2 h. Then, 800 μL of 5M HCl solution was spiked to the mixture to maintain Ag:Cl molar ratio of <1.0. The AgCl-SPAC composite was kept mixing for one more hour. The mixture was left to settle and the supernatant (ethanol) was decanted and replaced by DDW. A rotary evaporator was used to remove any residual ethanol. Excess amounts of NaCl were added to the decanted ethanol, and no white precipitate (AgCl) was formed that indicated the total transformation of AgNO₃ in the composite. It should be noted that AgCl is sensitive to light and heat. Therefore, centrifugation was avoided, because it requires resuspension via sonication that would heat and convert AgCl particles to metallic silver. Finally, the concentration of the AgCl-SPAC composite in the final slurry was determined by drying a known volume of the solution at 105 °C overnight and measuring the weight of the solid mass. Silver concentrations in the solutions were measured using plasma-atomic emission spectrometry (ICP-AES).

Nitrogen gas adsorption was performed at 77 °K with an ASAP 2020 analyzer (Micromeritics Instrument Corp. U.S.). Then, Brunauer–Emmett–Teller (BET) equation and density functional theory (DFT) were used to determine the specific surface area and pore size distributions, respectively. The particle size distribution was measured using a Laser Diffraction Particle Size Analyzer, SALD-2300, Shimadzu Corporation, Japan. Scanning electron microscopy (SEM) imaging and elemental compositions of all samples was carried out in the SE mode using energy-dispersive X-ray (EDX) measurement with a Hitachi HD-2000 STEM at an operating voltage of 150 kV. X-ray diffraction (XRD) diffractograms were acquired with Cu $K\alpha_{1,2}$ (1.5406 Å), Ni-filtered radiation using a Bruker D8 Advance instrument equipped with a LynxEye PSD detector. Diffractograms were collected from 15 to 70° 2 θ with 0.03° 2 θ step size and 8 s time step, while the sample was spun at 15 rpm. The

Table 1
Characteristics of SPAC used in this study.

Sample	Product name	Origin material	Silver content (%)	Specific surface area (m ² /g)	Total pore volume (cm ³ /g)	Particle size (μm) (mean \pm STDV)
SPAC1	Filtrisorb 400 [F400]	Bituminous Coal	—	1047	0.58	1.68 \pm 0.16
AgCl-SPAC1			34.3 ^a	658	0.45	1.75 \pm 0.18
SPAC2	Hydrodarco B [HDB]	Coconut Shell	—	555	0.56	1.58 \pm 0.16
AgCl-SPAC2			34.3 ^a	242	0.31	1.71 \pm 0.15
SPAC3	Aquacarb1230C [AQC]	Lignite Coal	—	1050	0.50	1.35 \pm 0.17
AgCl-SPAC3			34.3 ^a	636	0.59	1.54 \pm 0.17

^a Silver content were calculated a ratio of the molar mass of silver added to the system and the total mass of carbon and silver chloride.

divergence slit was set at 0.3° , antiscatter slit to 3° , primary and secondary Soller slits were 2.5° and a detector window opening was 2.71° . X-ray photoelectron spectra (XPS) were collected using a Kratos Axis Ultra^{DL} instrument. We used an AlK α monochromatic flux, with exciting radiation at 1486.6 eV and 150 W. The lens system of the photoelectron analyzer was set in the electrostatic mode to avoid rearranging and/or changing of the orientation of the magnetic particles during acquisition. Survey spectra were collected with the pass energy of 160 eV, and high-resolution spectra at 20 eV, with a resolution of 0.1 eV.

2.3. Adsorption studies

2.3.1. Kinetics experiments

Each data point of the kinetic experiments was determined by an individual batch experiment with an initial Br⁻ or I⁻ concentration of 1 mg/L and AgCl-SPAC dose of 10 mg/L at pH value of 6.5 ± 0.2 . Kinetics experiments were also run with mixtures of Br⁻ (1 mg/L) and I⁻ (1 mg/L) at Cl⁻ concentrations of 10 and 100 mg/L. All mixtures were shaken at a room temperature ($25 \pm 1^\circ\text{C}$) on an orbit shaker at 150 rpm. After certain time intervals, samples were collected, filtered (pre-washed 0.45 μm PES filter), and kept refrigerated until further measurements.

2.3.2. Effect of chloride and NOM on Br⁻ and I⁻ removal

The effects of Cl⁻ and NOM were evaluated in batch mode with an initial Br⁻ or I⁻ concentration of 1 mg/L and AgCl-SPAC concentration of 25 mg/L at pH value of 6.5 ± 0.2 . The tested Cl⁻ concentrations were 0.5, 10, 50, 100, 150, 200, 300, and 400 mg/L to cover challenging range of water quality conditions. Two NOM isolates collected from the influent of different drinking water treatment plants in South Carolina using reverse osmosis and followed by resin fractionation during a previous study were used (Song et al., 2009). The tested NOM solutions had different specific ultraviolet absorbance (SUVA₂₅₄) of 4.9 and 1.7 L/mg.m, and they were used to evaluate the performance of AgCl-SPAC under varying NOM concentration with DOC at 1, 2, 4, and 8 mg/L. The composite performance was also tested in four different surface waters and one groundwater with spiked Br⁻ and I⁻ concentrations of 1 and 0.1 mg/L, respectively. It should be highlighted the groundwater was not spiked with Br⁻, because it was collected from a site with high Br⁻ level. The Cl⁻ concentrations were adjusted to 50 mg/L in all waters to compare the effect of the water source. The characteristics of all waters were summarized in Table 2.

2.4. Chlorination and chloramination experiments

Chlorine and chloramine demand tests were performed under

uniform formation conditions (UFC) to determine the initial chlorine and chloramine concentrations that results in chlorine and chloramine residuals after 24 h of 1.0 mg/L and 2.0 mg/L as Cl₂, respectively. For chlorination, samples were buffered at pH 7.5 and spiked with target pre-determined concentrations using sodium hypochlorite stock solution (5% available free chlorine; 1 g/L). Chloramination was performed using preformed chloramine at pH 7.5. Preformed chloramine stock solution (1 g/L as Cl₂) was prepared by titrating ammonium sulfate stock solution. Samples were analyzed for residual chlorine and chloramine according to the DPD colorimetric method (SM 4500-Cl G). Residual chlorine and chloramine was quenched with a stoichiometric amount of ascorbic acid (99%) obtained from Sigma–Aldrich (St. Louis, MO) and ACS grade Na₂SO₃ purchased from EMD Millipore Co. (Billerica, MA), respectively. After quenching, samples were extracted and analyzed for THMs, I-THMs, HAAs, halogenated acetonitrile (HAN), and total organic halogen (TOX; i.e., TOCl, TOBr, and TOI). A detailed description of extraction and analysis of DBPs and TOX can be found in the supporting information section as well as in our previous publications (Text S1 in SI) (Ersan et al., 2019; Liu et al., 2018).

Cytotoxicity of the chlorinated and chloraminated water samples was calculated using cytotoxicity index values obtained from the previous literature (Table S2). In brief, the calculations were performed by dividing the molar concentration of each species by the cytotoxicity index values (%C¹/₂, given as M), obtained from the literature. The analytical methods used in this study and their minimum detection limits (MDL) are listed in the supporting information (Table S1).

3. Results and discussion

3.1. Microscopic and spectroscopic characterization of AgCl-SPAC

Micrographs of the SPAC and AgCl-SPAC1 samples are shown in Fig. 1A and B, respectively, that confirm the presence and the attachment of AgCl particles on the carbon surface. EDX analysis indicated that the composite contains C, Ag, and Cl (Fig. 1C). As shown in Fig. 2, SPAC showed XRD diffraction peaks at ~ 26 and $54^\circ 2\theta$ that are attributed to the diffractions from the graphite-like structure (Oh et al., 2015). However, AgCl-SPAC showed four diffraction peaks located at 27.8° , 32.2° , 46.2° and 57.5° that were assigned to cubic AgCl (JCPDS no. 31–1238) and indexed to the (111), (200), (220) and (222) crystal planes, respectively (Liang et al., 2018). These observations were further confirmed using XPS (Fig. 2B, S2 and Table S3). From the XPS survey spectrum it was possible to detect the presence of Ag (0.4%) and Cl (0.6%). Some residuals of Si, Al, S, Zr and N were also detected in the starting SPAC material and in all samples. In the Ag 3d spectrum is possible to

Table 2
Source water characteristics.

Water Source	Code	Water Type	Br ⁻ (mg/L) ^a	I ⁻ (mg/L) ^a	Cl ⁻ (mg/L) ^a	NO ₃ ⁻ (mg/L)	SO ₄ ⁻ (mg/L)	DOC (mg/L)	UV ₂₅₄ (cm ⁻¹)	SUVA ₂₅₄ (L/mg.m)
Groundwater ^b	GW	Natural Water	2.00 [*]	0.10	51.21	0.50	34.55	0.78	0.013	1.72
Treated Surface water ^c	TSW		1.06	0.10	48.79	0.15	47.06	2.09	0.056	2.67
Lake Water ^d	LW		1.04	0.11	49.61	<LoD	4.97	1.52	0.038	2.50
AOM-impacted Lake Water ^e	AOM		1.05	0.11	48.45	<LoD	0.04	2.01	0.045	2.24
EfOM-impacted Lake Water ^f	EfOM		1.07	0.10	47.66	3.77	5.99	1.53	0.035	2.30
CH-HPO ^g	HS	Isolated NOM Powder	1.06	1.01	1.52	<LoD	<LoD	–	–	4.90
CH-TPH ^g	LS		1.04	1.06	1.51	<LoD	<LoD	–	–	1.70
No NOM	–	DDW	1.05	0.10	52.97	<LoD	<LoD	<LoD	–	–

^a These are adjusted concentration by spiking known amounts of NaCl, NaBr, or NaI solutions ^b Groundwater was collected from a site with high Br⁻ concentrations ^{*} This Br⁻ concentration is Not spiked. ^c Treated water effluent from Myrtle Beach water treatment plant. ^d Water from Lake Hartwell, South Carolina. ^e AOM was prepared as reported in our previous study and mixed with water from Lake Hartwell by volume ration of 1:10 (AOM:Lake water). ^f Wastewater effluent was collected from a wastewater treatment plant and mixed with water from Lake Hartwell by volume ration of 1:10 (EfOM:Lake water). ^g The water was collected from the influents to drinking water treatment plants in Charleston, South Carolina. DDW: distilled-deionized water.

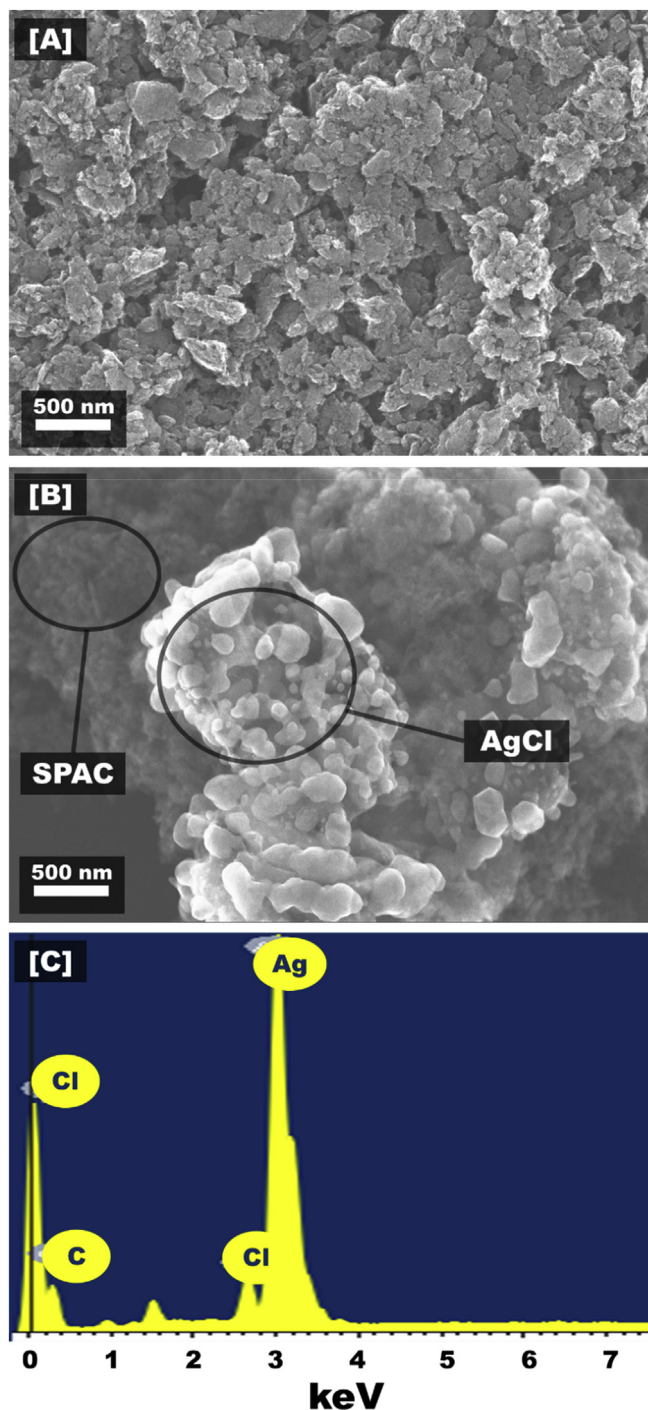


Fig. 1. SEM micrographs of [A] SPAC1 and [B] AgCl-SPAC1. [C] EDX spectra for AgCl-SPAC1.

identify only one doublet (Ag 3d_{5/2} at 366.8 eV, Ag 3d_{3/2} at 372.8 eV) that is assigned to Ag in AgCl while formation of a stable silver carbide (Ag-C) bond was excluded (Boukhvalov et al., 2018). The C 1s spectra are similar for all the 4 samples and were fitted with 6 different components: the peak at 284.6 eV stems from sp²/sp³ non-functionalized carbon (C-C, C=C, C-H), the peak at 286.7 eV originates from C-O bond, the peak at 288.3 eV from C=O bond while the peak at 289.5 eV is attributed to O-C=O bond. Peaks at 291.0 eV and 293.4 eV are typical of shake-up satellite (Papirer et al., 1994). The Cl 2p spectrum shows at least two components, the first

one is attributed to Cl⁻, and is characterized by a doublet, with a Cl 2p_{3/2} peak located at 197.05 eV, while the second doublet at 199.85 eV originates from Cl₂⁻ (Strydom et al., 1990). The same analysis were also performed on the spent composites after treatment as described in the following sections.

3.2. Removal efficiency of Br⁻ and I⁻ by adsorption on AgCl-SPAC

Preliminary experiments were run to evaluate the removal of Br⁻ and I⁻ using the three composites (i.e., AgCl-SPAC1, AgCl-SPAC2, and AgCl-SPAC3). As shown in Fig. S1, all composites exhibited similar removal efficiencies for Br⁻ and I⁻ in the presence and in the absence of spiked Cl⁻ concentrations at 100 mg/L. These results indicated that the SPAC types and characteristics had minimal effect on the composites' performance. Thus, all experiments in the subsequent sections were run with only AgCl-SPAC1. All samples were measured after treatment using ICP-AES and no silver leaching was observed.

3.2.1. Br⁻ and I⁻ removal kinetics

Fig. 3 depicts the fast removal kinetics of Br⁻ and I⁻ by AgCl-SPAC1 with equilibrium times at 150 s and <10 s, respectively. The applied AgCl-SPAC1 dose was only 10 mg/L, which reflects the superior performance of our composite compared to other previously tested Ag-based materials. For instance, Rajaieian et al. (2018) have recently reported on the kinetics of Br⁻ removal using silver impregnated activated carbon (SIAC; Norit AG, Cabot Norit) at initial Br⁻ concentration of 1–6 mg/L and SIAC dose of 800 mg/L. Although they have used adsorbent dose >30 times higher than our tested concentration, the equilibrium time using SIAC was in the range of 120–180 min (i.e., 50–60 times longer than AgCl-SPAC). In addition (Sanchez-Polo et al., 2007), developed Ag-doped carbon aerogels and tested the removal kinetics of Br⁻ and I⁻ (100 µg/L) at composite dose of 1000 mg/L. Despite the high dose in their study, the removal did not reach an equilibrium within their tested experiment time (i.e., 60–70 min). Similarly, the equilibrium time for Br⁻ removal using silver-loaded porous carbon spheres was in the range of 240–720 min (Gong et al., 2013).

At the end of the kinetics experiments, the composites were collected, dried, and tested using XRD and XPS. Fig. 2 confirms the formation of AgBr (diffraction peaks at 31 and 44 °2θ) and AgI (diffraction peaks at 25, 33, 43, 48 and 59 °2θ) (Lee et al., 2000; Zang and Farnood, 2008). These observations are in line with the XPS analysis as summarized in Table S3, Fig. 2B and S2. For AgBr-SPAC, Ag surface concentration is 0.6% and Br 0.8% while for AgI, Ag is 1.5% and I is 16%. For AgBr-SPAC the peak position of Ag 3d_{5/2} is 367.5 eV and Br 3d_{5/2} is 67.7 eV confirming the formation of AgBr. The presence of AgI for AgI-SPAC is supported by the Ag 3d_{5/2} peak at 368.0 eV and I 3d_{5/2} peak at 619.1 eV (Strydom et al., 1991).

In this study, we also report on the effect of coexisting anions on the halides removal kinetics by AgCl-SPAC1. As shown in Fig. 3, only a slight change in the kinetics of the simultaneous removal of Br⁻ and I⁻ was observed. Further, the effect of two Cl⁻ concentrations (10 and 100 mg/L) on the removal kinetics was evaluated. The Br⁻ removal was slower only when Cl⁻ concentration was elevated to 100 mg/L with an observed equilibrium time of 10–15 min. Meanwhile, elevating Cl⁻ concentration did not affect the removal speed of I⁻ using AgCl-SPAC1. To the best of our knowledge, no similar kinetics data (i.e., under challenging conditions) has been reported in the literature for other Ag-based sorbents.

3.2.2. Effect of chloride and NOM on Br⁻ and I⁻ removal

Previous studies have indicated high Cl⁻ concentrations as a limiting factor for Br⁻ removal (Chen et al., 2017; Gan et al., 2018; Kidd et al., 2018). In our study, the removal of Br⁻ and I⁻ by AgCl-

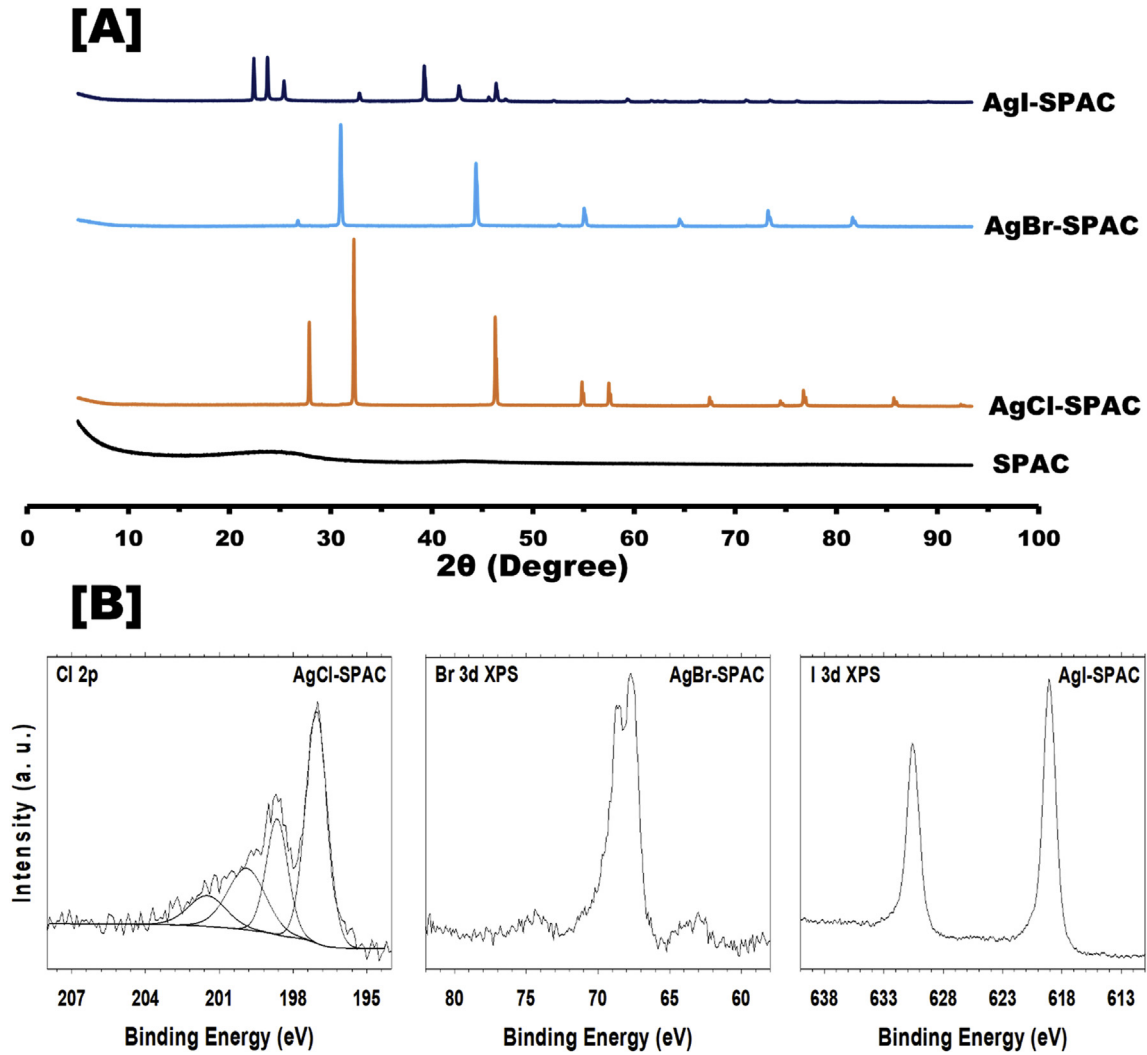


Fig. 2. [A] XRD traces of SPAC1 and AgCl-SPAC1 as well as AgBr-SPAC1 and AgI-SPAC1 (i.e., after treatment) and [B] XPS Cl 2p spectrum for AgCl-SPAC, Br 3d spectrum for AgBr-SPAC and I 3d spectrum for AgI-SPAC.

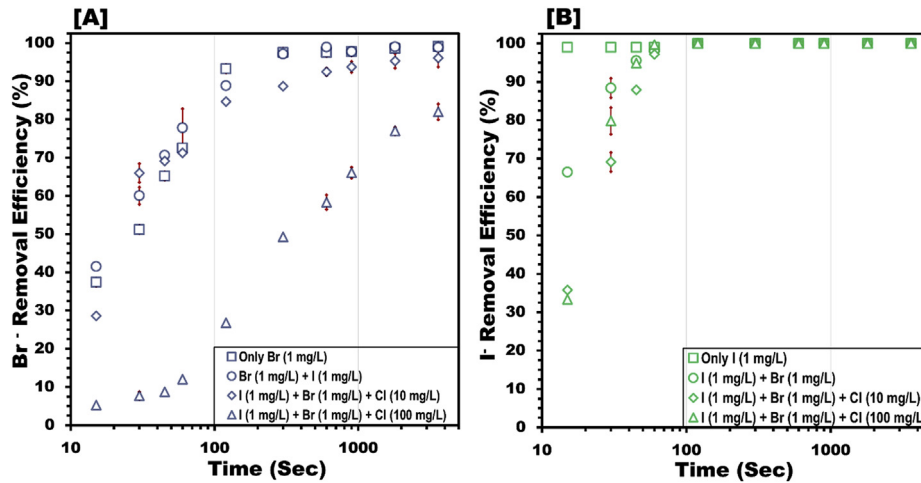


Fig. 3. Kinetics experiments for [A] Br⁻ and [B] I⁻ using AgCl-SPAC1. Experiments were run in single solute experiments and in Cl⁻ challenging conditions. AgCl-SPAC1 dose = 10 mg/L and pH = 6.5. Values are means of data from triplicate experiments and the standard deviation indicated by vertical error bars.

SPAC1 was evaluated under 8 different Cl^- concentrations up to 400 mg/L, which corresponded to molar ratios of $\text{Cl}^-:\text{Br}^-$ and $\text{Cl}^-:\text{I}^-$ up to 900 and 1450, respectively. As illustrated in Fig. 4A, AgCl-SPAC1 maintained very high I^- removal efficiency (>90%) at all tested conditions. Concurrently, the Br^- removal efficiencies were 85–97% at Cl^- concentrations up to 200 mg/L. When Cl^- concentration was raised to 300–400 mg/L, the Br^- removal efficiencies decreased to 65–75%. Recently, Kidd et al. (2018) tested Ag-impregnated graphene oxide and showed Br^- removal efficiency of >90% under $\text{Cl}^-:\text{Br}^-$ mass ratio up to only 100 (the maximum tested Cl^- concentration was 20 mg/L). Besides, their material, in

comparison to AgCl-SPAC, needed extensive oxidation steps that would reflect on their applicability and environmental impact. The higher removal of I^- than Br^- using AgCl-SPAC was attributed to their differences in solubility, as the solubility product constants (K_{sp}) for AgBr and AgI are 5.35×10^{-13} and 8.52×10^{-17} , respectively. It should be noted that some previous studies suggested that higher levels of Cl^- ions causes the formation of 'bioavailable' AgCl_2^- ions (Silver, 2003). However, no silver was detected in our samples at high Cl^- concentration conditions.

NOM is ubiquitous in natural waters and wastewaters with orders of magnitudes higher concentrations than Br^- and I^- (Ateia

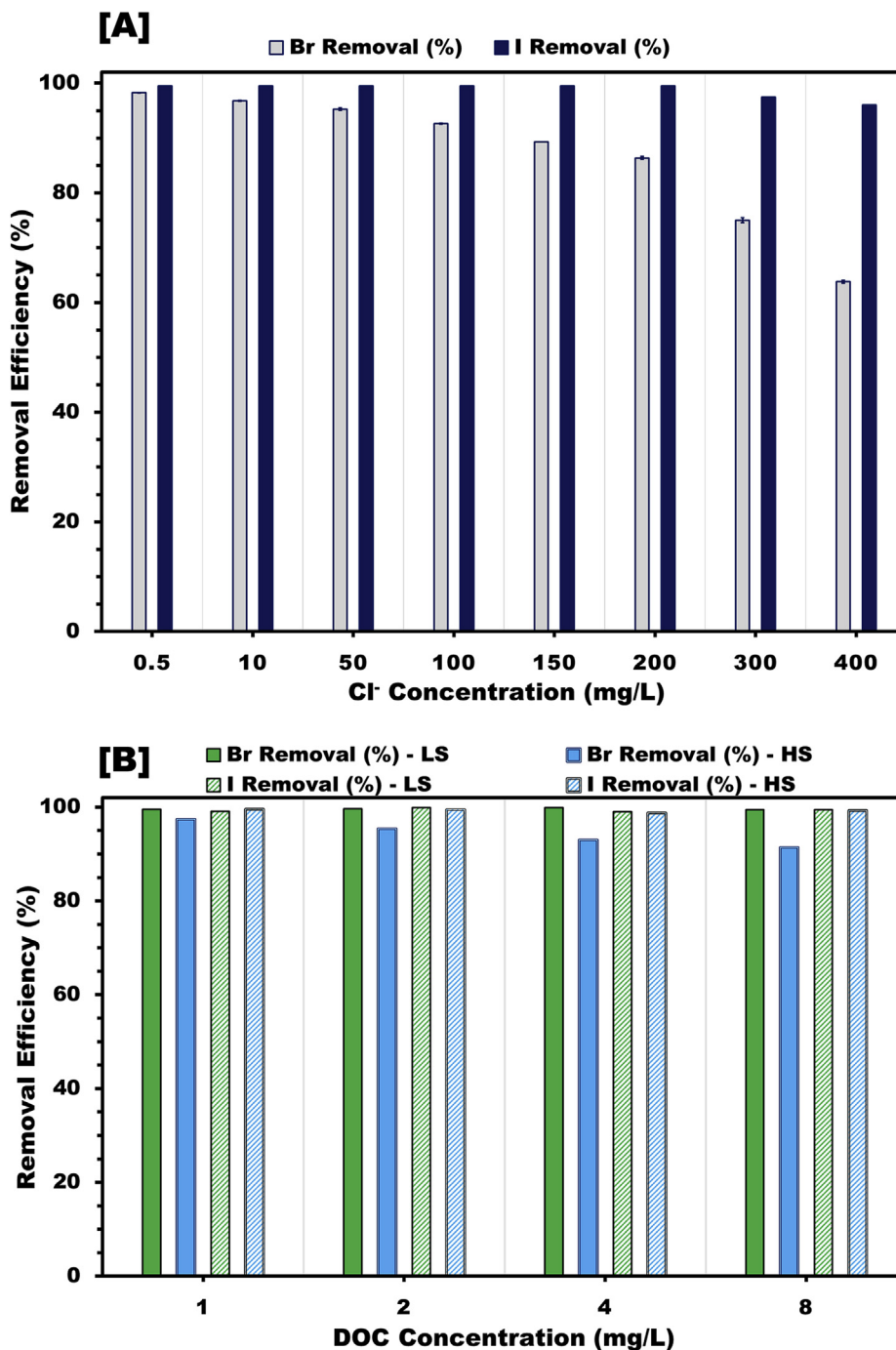


Fig. 4. Effect of [A] Cl^- , and [B] NOM on Br- and I- removal efficiency using AgCl-SPAC1. $[\text{Br}^-]_0 = 1 \text{ mg/L}$, $[\text{I}^-]_0 = 1 \text{ mg/L}$, pH = 6.5, AgCl-SPAC dose = 25 mg/L, and reaction time = 2 h. LS: low SUVA_{254} NOM and HS: high SUVA_{254} NOM.

et al., 2017a; Shimizu et al., 2018). The effects of NOM concentration (2–16 mg-NOM/L) and type (i.e., high $SUVA_{254}$ and low $SUVA_{254}$) on Br^- and I^- removal by AgCl-SPAC1 are shown in Fig. 4B. The removal efficiencies of I^- were >95.5% at all tested conditions using both NOM solutions (i.e., DOC = 1–8 mg/L). The Br^- removal was not affected by the elevated concentrations of low $SUVA_{254}$ NOM, however, the removal efficiency decreased by 2, 4, and 7% when the concentration of high $SUVA_{254}$ NOM increased to 2, 4, and 8 mg-DOC/L. The previously tested Ag-based materials were severely impacted with the presence of NOM by two main hypothesized mechanisms: 1) high $SUVA_{254}$ NOM have high molecular size that can cause blockage of the pores, and 2) NOM is negatively charged and can interact with Ag^+ (Ateia et al., 2017b; Gabelich et al., 2002; Sanchez-Polo et al., 2007). The main removal mechanism of Br^- and I^- by AgCl-SPAC1 is by ion exchange which is reflected on its selectivity and superior effectiveness compared to previous materials. We have further examined the performance of AgCl-SPAC1 in four different spiked surface waters and one groundwater (Table 2). The initial $Br^-:I^-$ mass ratio was 10 in all surface waters and was 20 in the groundwater due to the high Br^- concentration in the source. The removal efficiencies of Br^- and I^- from the groundwater were 94 ± 3 and 91%, respectively. Besides, except for lake water impacted with a treated wastewater effluent organic matter (EfOM), the removal of Br^- and I^- from all tested surface waters in this study were in the range of 84–86 and 95–97%, respectively (Fig. 5). The EfOM-impacted lake water reduced the Br^- and I^- removal by 12% and 7%, respectively. This reduction might be attributed to the presence of other constituents in the treated wastewater. The impact of Br^- and I^- removal from all tested waters on the subsequent DBPs formation was further discussed in the following section.

3.2.3. The impact of AgCl-SPAC on THMs, HAAs, and HAN formation and speciation

For the tested five water sources, the impact of AgCl-SPAC1 treatment on the DBP formation and speciation was evaluated under both chlorination and chloramination conditions. Fig. 6 shows the formation and speciation of DBPs (i.e. THMs, HAAs,

and HANs) in the studied waters before and after AgCl-SPAC treatment. THMs formation in LW, GW, TSW, EfOM and AOM waters were 46.0, 57.2, 193.1, 137.5, 174.6 $\mu\text{g/L}$, respectively (Fig. 6A). Among the studied waters, higher total formation of THMs were observed in TSW, EfOM and AOM, sources as compared to LW and GW sources. The observed differences in total formations can be explained by the differences in organic matter concentration (DOC) and type ($SUVA_{254}$), which can alter the formation and speciation of both Cl-THMs and Br-THMs. For example, whereas both TSW and AOM had similar DOC concentrations, their total THM formations were slightly different. TSW had higher $SUVA_{254}$ value than AOM (Table 2), which can explain THM formation difference. While the GW's DOC concentration and $SUVA_{254}$ value were less than LW, the total THMs formations were similar. The reason for high formation in GW is the higher initial Br^- concentration (Table 2). Although, the tested waters had varying $SUVA_{254}$, no difference was observed among BSF_{THM} values (Table S4). This might be attributed to the relatively high initial bromide concentration ($[Br^-]_0 = 12.5 \mu\text{M}$), when compared to previous studies (Liu et al., 2018). The speciation of THMs in all studied water sources were in the order of $TBM > DBCM > DCBM > TCM$. In raw water samples, TBM was the dominant specie among the all THM species, which can be attributed to high initial concentration of Br^- in these waters. After AgCl-SPAC1 treatment, TBM concentrations significantly decreased by 82%, 94%, 96%, 79% and 94% from LW, GW, TSW, EfOM, and AOM background, respectively. While the concentration of TBM significantly decreased in the studied waters, the formation of TCM and DCBM increased due to shift in speciation from Br-THM to Cl/Br-THMs (Gan et al., 2018). The decrease in BSF_{THM} further shows the effectiveness of AgCl-SPAC1 treatment on the removal of Br-THMs, where 44%, 47%, 60%, 32%, 49% decrease in BSF_{THM} were observed in LW, GW, TSW, EfOM, and AOM background, respectively (Table S4).

Fig. 6B illustrates HAA formation and speciation of raw and treated waters by AgCl-SPAC1. Total HAA formation for LW, GW, TSW, EfOM and AOM waters were 106.3, 15.73, 44.3, 70.6, 88.6 $\mu\text{g/L}$, respectively. Although the initial DOC concentrations were similar (~2 mg/L) in TSW and AOM, the HAA formation was 2 times higher

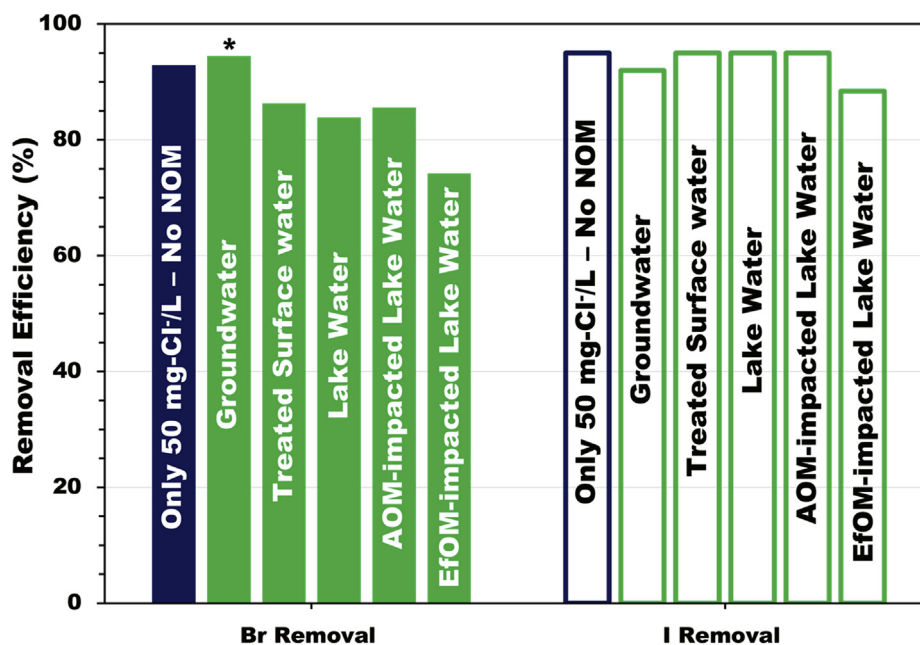


Fig. 5. Removal of Br^- and I^- from different water sources using AgCl-SPAC1. $[Cl^-]_0 = 50 \text{ mg/L}$, $[Br^-]_0 = 1 \text{ mg/L}$, $[I^-]_0 = 0.1 \text{ mg/L}$ * $[Br^-]_0 = 2 \text{ mg/L}$, AgCl-SPAC dose = 25 mg/L, and reaction time = 2 h.

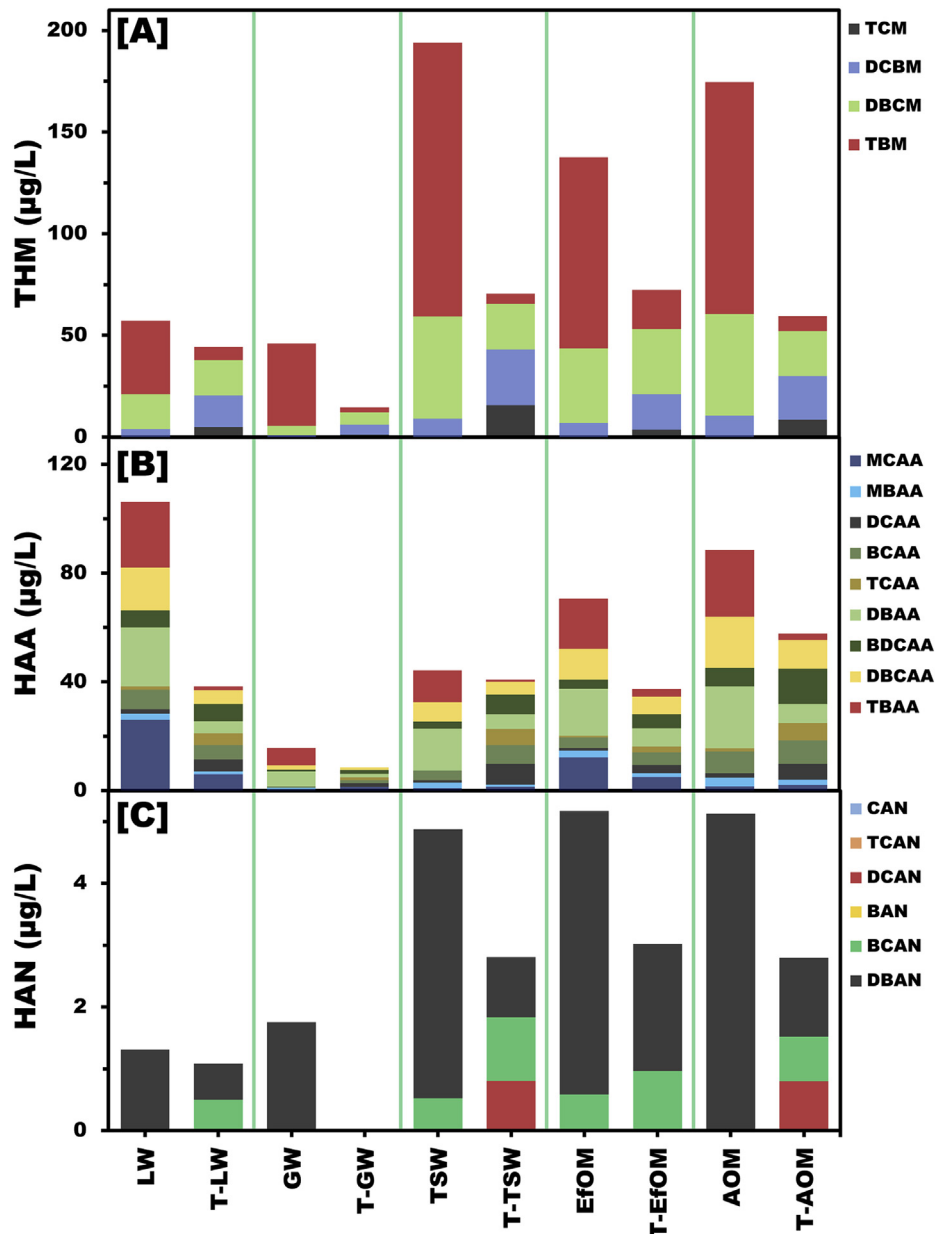


Fig. 6. Impact of AgCl-SPAC1 treatment on the formation and speciation of THMs, HAAs and HANs. Treatment conditions: $[Cl^-]_0 = 50 \text{ mg/L}$, $[Br^-]_0 = 1 \text{ mg/L}$, $[I^-]_0 = 0.1 \text{ mg/L}$, $[Br^-]_0 = 2 \text{ mg/L}$, AgCl-SPAC dose = 25 mg/L, and reaction time = 2 h. DBP experimental conditions: $[HOCl]_0 = 4.25 \pm 0.75 \text{ mg/L}$, $[Br]_0 = 1000 \text{ µg/L}$, $[I]_0 = 100 \text{ µg/L}$, pH = 7.5, $T = 21 \pm 1 \text{ °C}$, reaction time = 24 h.

in AOM than TSW. Br-HAAs (DBAA, BDCAA, DBCAA and TBAA) were the dominant species among the all detected HAA species. While 60% of HAAs species in all studied waters were Br-HAAs, they decreased significantly after AgCl-SPAC1 treatment for LW, GW, TSW, EfOM and AOM waters by 74.5%, 73.4%, 50.6%, 57.9%, and 55.0%, respectively. BSF_{HAA} values were also calculated and the results showed that BSF_{HAA} values decreased 41.8%, 64.6%, 59.3%, 30.0%, and 46.2% from LW, GW, TSW, EfOM, and AOM background, respectively (Table S4).

Fig. 6C shows the formation, speciation and removal of HANs by AgCl-SPAC. Total HAN formation ranged from 1.3 to 10.9 µg/L. While total HAN formation of LW and GW were below 2.0 µg/L, TSW, EfOM and AOM had similar HAN formations (4.9, 5.2, 5.2 µg/L, respectively). The speciation of HANs in all studied water sources were in the order of DBAN > BCAN > DCAN (CAN, TCAN and BAN were not

detected). The observed higher concentration of DBAN among the all HAN species attributed to high initial concentration of Br^- in these waters. Total HAN removals in TSW, EfOM and AOM were 42.5%, 41.6%, 45.4%, respectively. After AgCl-SPAC1 treatment, speciation of HANs shifted from Br-HAN (DBAN) to Cl/Br-HANs (DCAN and BCAN), which can be linked to reduced concentration of Br in the background waters. Because of very low or no formation of chlorinated HANs BSF_{HAN} values were higher than 0.9 for all waters. Removal percentages of DBAN for LW, GW, TSW, EfOM and AOM were 55.5%, >99%, 77.7%, 55.2%, 75.1% respectively which also confirms the Br^- selectivity of this SPAC. BSF_{HAN} decrease calculated as 26.2%, >99%, 53.2%, 12.7%, 52.3% from LW, GW, TSW, EfOM, and AOM background, respectively (Table S4). Fig. 7 shows the total formation and removal of organic halides (TOCl, UTOCl, TOBr, and UTOBr) from the studied water sources after AgCl-SPAC treatment.

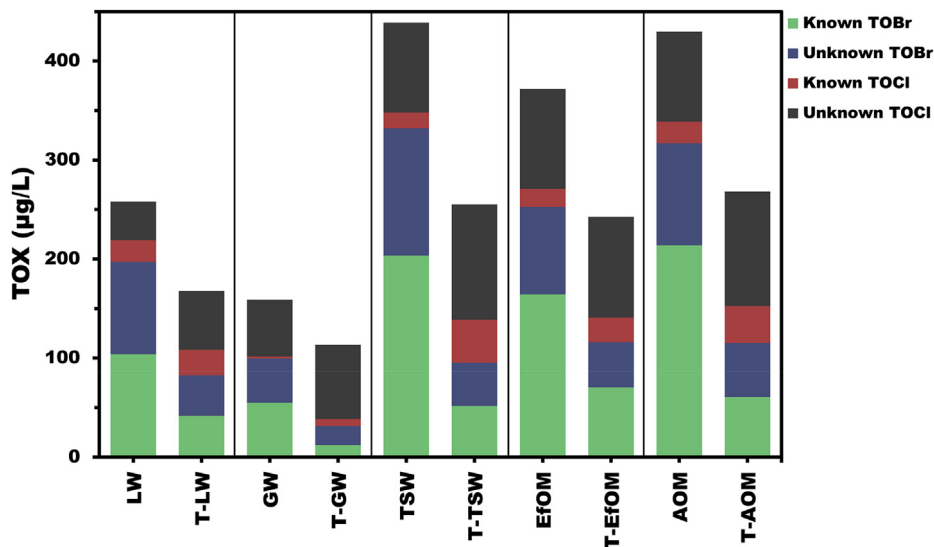


Fig. 7. Impact of AgCl-SPAC1 treatment on the formation and speciation of TOX (TOCI, TOBr). Treatment conditions: $[Cl^-]_0 = 50$ mg/L, $[Br^-]_0 = 1$ mg/L, $[I^-]_0 = 0.1$ mg/L * $[Br^-]_0 = 2$ mg/L, AgCl-SPAC dose = 25 mg/L, and reaction time = 2 h. DBP experimental conditions: $[HOCl]_0 = 4.25 \pm 0.75$ mg/L, $[Br]_0 = 1000$ µg/L, $[I]_0 = 100$ µg/L, pH = 7.5, $T = 21 \pm 1$ °C, reaction time = 24 h.

Total TOX formation for LW, GW, TSW, EfOM, and AOM waters were 258, 159, 439, 372, and 430 µg/L, respectively. In Fig. 7, the known TOX consist of measured THMs, HAAs, and HANs and the unknown TOX calculated by subtracting known TOX from total TOX. Overall, in percent wise, 49%, 36%, 50%, 49%, and 55% of the total TOX comprises of known TOX in LW, GW, TSW, EfOM and AOM, respectively. The application of AgCl-SPAC treatment was effective in reducing both known and unknown TOBr by 58.1%, 68.4%, 71.3%, 54.1%, and 63.6% from LW, GW, TSW, EfOM, and AOM, respectively.

Experiments were also conducted under chloramination conditions to evaluate the impact of AgCl-SPAC treatment on I-THMs removal, and results were given in Fig. 8. Total I-THM formations for LW, GW, TSW, EfOM, and AOM waters were 17.0, 32.1, 14.0, 28.3, and 8.8 µg/L, respectively. Among the detected species, TIM (iodoform) was the most dominant species (Fig. 8), due to the high initial I^- concentration of 100 µg/L in all source waters. The treatment

results showed that AgCl-SPAC was also very effective to remove I-THMs from water, where total I-THM removals in LW, GW, TSW, EfOM, and AOM were 96.9%, 92.5%, 96.6%, 91.5%, and >99%, respectively (Fig. 8). The results indicate that AgCl-SPAC1 was effective in removing both brominated and iodinated DBPs simultaneously, which brings extra benefit when the formation of Br/I-DBPs is of concern during water treatment.

In addition, the impact of AgCl-SPAC1 treatment on the calculated cytotoxicity of raw and treated samples was investigated. Based on the measured DBPs, the total calculated cytotoxicity values for the studied raw waters were in the order of AOM > TSW > EfOM > LW > GW (Fig. S3A). The results also indicated that HANs (i.e., DBPs with the highest cytotoxicity index values within the detected DBP classes in this study) controlled the calculated cytotoxicity of the samples regardless of their lower formations. After AgCl-SPAC treatment, calculated cytotoxicity

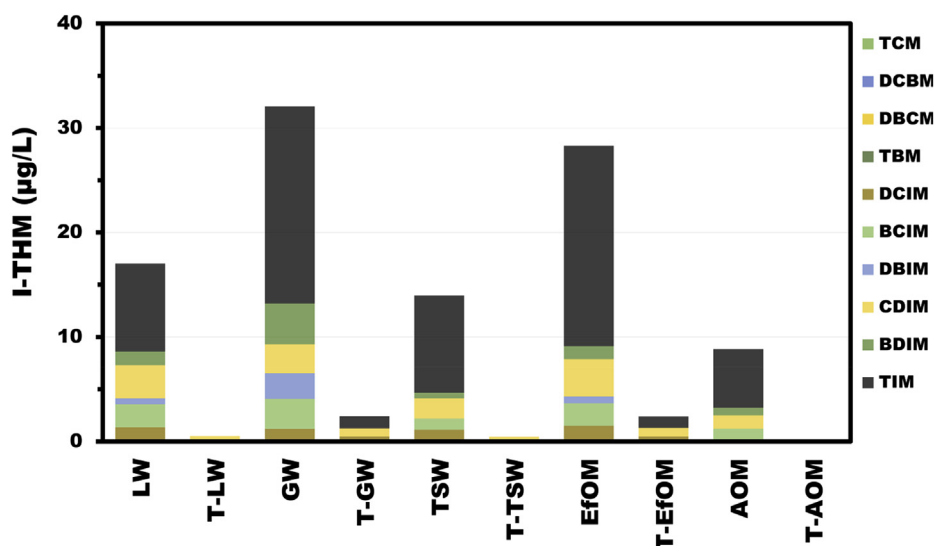


Fig. 8. THM and I-THM formation and speciation of raw and treated waters after chloramination. Treatment conditions: $[Cl^-]_0 = 50$ mg/L, $[Br^-]_0 = 1$ mg/L, $[I^-]_0 = 0.1$ mg/L * $[Br^-]_0 = 2$ mg/L, AgCl-SPAC dose = 25 mg/L, and reaction time = 2 h.

values decreased by 23.3%, 47.1%, 59.3%, 27.4%, and 59.2% from LW, GW, TSW, EfOM, and AOM background, respectively. Similarly, under chloramination oxidation, the total calculated cytotoxicity values for the studied waters were in the order of EfOM > GW > TSW > LW > AOM (Fig. S3B). After AgCl-SPAC1 treatment, calculated cytotoxicity values decreased by 99.8%, 93.8%, 99.8%, 94.1%, and >99% from LW, GW, TSW, EfOM, and AOM waters, respectively.

4. Conclusions

This study explored, for the first time, the use of AgCl-SPAC composite for the removal of Br⁻ and I⁻ from four different surface waters and one groundwater to control the formation of the Br-DBPs and I-DBPs. The proposed synthesis method, unlike previously reported studies, is simple and environmental-friendly, as it does not require any acid oxidation steps. In addition, the resulting composite showed rapid and selective removal for Br⁻ and I⁻ under typical challenging background water conditions (i.e., Cl⁻ = 0.5–400 mg/L, and NOM = 1–8 mg-DOC/L). A significant decrease in the formation of the subsequent DBPs (THMs, HAAs, and HANs) and the total organic halogens (TOX) was observed after the application of AgCl-SPAC1 to all tested waters under UFC conditions. In addition, similar reduction was shown in the calculated BSF and calculated cytotoxicity of all waters. In full-scale water treatment plants, AgCl-SPAC can be used in the same way as regular SPAC (i.e., the addition to a mixed tank preceding a filter such as an ultrafiltration) (Takaesu et al., 2019). Thus, the continuous and/or seasonal integration of such novel composites in water treatment plants can represent an alternative strategy to control the formation of brominated and/or iodinated DBPs.

Author agreement

This is to certify that all authors have seen and approved the final version of the manuscript being submitted. They warrant that the article is the authors' original work, hasn't received prior publication and isn't under consideration for publication elsewhere.

Declaration of interests

The authors declare that they have no known competing financial interests or personal relationships that could have appeared to influence the work reported in this paper.

Acknowledgments

This work was supported, in part, by a research grant from the National Science Foundation (CBET 1511051). We would like to thank Ms. Meryem Soyuloglu for the preparation of AOM.

Appendix A. Supplementary data

Supplementary data to this article can be found online at <https://doi.org/10.1016/j.watres.2019.03.028>.

References

Amy, G., Siddiqui, M., Zhai, W., DeBroux, J., Odem, W., 1993. Nationwide Survey of Bromide Ion Concentrations in Drinking Water Sources.

Ateia, M., Apul, O.G., Shimizu, Y., Muflihah, A., Yoshimura, C., Karanfil, T., 2017a. Elucidating adsorptive fractions of natural organic matter on carbon nanotubes. *Environ. Sci. Technol.* 51 (12), 7101–7110.

Ateia, M., Ran, J., Fujii, M., Yoshimura, C., 2017b. The relationship between molecular composition and fluorescence properties of humic substances. *Int. J. Environ.*

Sci. Technol. 1–14.

Bo, L., 2008. Electrolytic Cell and Process for Removal of Bromide Ions and Disinfection of Source Waters Using Silver Cathode And/or Dimensionally Stable Anode (DSA): a Process for the Reduction of Disinfectant/Disinfection Byproducts in Drinking Water. Google Patents.

Boukhalvalov, D., Zhidkov, I., Kurmaev, E., Fazio, E., Cholakh, S., D'Urso, L., 2018. Atomic and electronic structures of stable linear carbon chains on Ag-nanoparticles. *Carbon* 128, 296–301.

Chen, C., Apul, O.G., Karanfil, T., 2017. Removal of bromide from surface waters using silver impregnated activated carbon. *Water Res.* 113, 223–230.

Dorji, P., Choi, J., Kim, D.L., Phuntsho, S., Hong, S., Shon, H.K., 2018. Membrane capacitive deionisation as an alternative to the 2nd pass for seawater reverse osmosis desalination plant for bromide removal. *Desalination* 433, 113–119.

Ersan, M.S., Liu, C., Amy, G., Karanfil, T., 2019. The interplay between natural organic matter and bromide on bromine substitution. *Sci. Total Environ.* 646, 1172–1181.

Gabelich, C.J., Tran, T.D., Suffet, I.M., 2002. Electrosorption of inorganic salts from aqueous solution using carbon aerogels. *Environ. Sci. Technol.* 36 (13), 3010–3019.

Gan, W., Venkatesan, A.K., Apul, O.G., Perreault, F., Yang, X., Westerhoff, P., 2018. Bromide and Other Halide Ion Removal from Drinking Waters Using Silver-Amended Coagulation. *Journal-American Water Works Association*.

Gong, C., Zhang, Z., Qian, Q., Liu, D., Cheng, Y., Yuan, G., 2013. Removal of bromide from water by adsorption on silver-loaded porous carbon spheres to prevent bromate formation. *Chem. Eng. J.* 218, 333–340.

Ho, P.C., Kraus, K.A., 1981. Adsorption on inorganic materials—VIII: adsorption of iodide on AgCl-filled carbon. *J. Inorg. Nucl. Chem.* 43 (3), 583–587.

Hoskins, J.S., Karanfil, T., Serkiz, S.M., 2002. Removal and sequestration of iodide using silver-impregnated activated carbon. *Environ. Sci. Technol.* 36 (4), 784–789.

Jones, D.B., Saglam, A., Song, H., Karanfil, T., 2012. The impact of bromide/iodide concentration and ratio on iodinated trihalomethane formation and speciation. *Water Res.* 46 (1), 11–20.

Jones, D.B., Saglam, A., Triger, A., Song, H., Karanfil, T., 2011. I-THM formation and speciation: preformed monochloramine versus prechlorination followed by ammonia addition. *Environ. Sci. Technol.* 45 (24), 10429–10437.

Kidd, J., Barrios, A., Apul, O., Perreault, F., Westerhoff, P., 2018. Removal of bromide from surface water: comparison between silver-impregnated graphene oxide and silver-impregnated powdered activated carbon. *Environ. Eng. Sci.* 35, 988–995.

Kimbrough, D.E., Suffet, I., 2002. Electrochemical removal of bromide and reduction of THM formation potential in drinking water. *Water Res.* 36 (19), 4902–4906.

Lee, J.-S., Adams, S., Maier, J., 2000. A mesoscopic heterostructure as the origin of the extreme ionic conductivity in AgI: Al₂O₃. *Solid State Ionics* 136, 1261–1266.

Liang, X., Wang, P., Li, M., Zhang, Q., Wang, Z., Dai, Y., Zhang, X., Liu, Y., Whangbo, M.-H., Huang, B., 2018. Adsorption of gaseous ethylene via induced polarization on plasmonic photocatalyst Ag/AgCl/TiO₂ and subsequent photodegradation. *Appl. Catal. B Environ.* 220, 356–361.

Liu, C., Ersan, M.S., Plewa, M.J., Amy, G., Karanfil, T., 2018. Formation of regulated and unregulated disinfection byproducts during chlorination of algal organic matter extracted from freshwater and marine algae. *Water Res.*

Oh, I., Kim, M., Kim, J., 2015. Controlling hydrazine reduction to deposit iron oxides on oxidized activated carbon for supercapacitor application. *Energy* 86, 292–299.

Papirer, E., Lacroix, R., Donnet, J.-B., Nanse, G., Fioux, P., 1994. XPS Study of the halogenation of carbon black-part 1. Bromination. *Carbon* 32 (7), 1341–1358.

Partlan, E., Davis, K., Ren, Y., Apul, O.G., Mefford, O.T., Karanfil, T., Ladner, D.A., 2016. Effect of bead milling on chemical and physical characteristics of activated carbons pulverized to superfine sizes. *Water Res.* 89, 161–170.

Plewa, M.J., Wagner, E.D., Richardson, S.D., 2017. TIC-Tox: a preliminary discussion on identifying the forcing agents of DBP-mediated toxicity of disinfected water. *J. Environ. Sci.* 58, 208–216.

Polo, A., Lopez-Peñalver, J., Rivera-Utrilla, J., Von Gunten, U., Sánchez-Polo, M., 2017. Halide removal from waters by silver nanoparticles and hydrogen peroxide. *Sci. Total Environ.* 607, 649–657.

Polo, A., Velo-Gala, I., Sánchez-Polo, M., Von Gunten, U., López-Peñalver, J., Rivera-Utrilla, J., 2016. Halide removal from aqueous solution by novel silver-polymeric materials. *Sci. Total Environ.* 573, 1125–1131.

Rajaeian, B., Allard, S., Joll, C., Heitz, A., 2018. Effect of preconditioning on silver leaching and bromide removal properties of silver-impregnated activated carbon (SIAC). *Water Res.* 138, 152–159.

Richardson, S., 2014. Formation of DBPs: State of the Science, vol.1155. AMER CHEMICAL SOC, 16TH ST, NW, WASHINGTON, DC 20036 USA.

Richardson, S.D., Plewa, M.J., Wagner, E.D., Schoeny, R., DeMarini, D.M., 2007. Occurrence, genotoxicity, and carcinogenicity of regulated and emerging disinfection by-products in drinking water: a review and roadmap for research. *Mutat. Res. Rev. Mutat. Res.* 636 (1), 178–242.

Sánchez-Polo, M., Rivera-Utrilla, J., Salhi, E., Von Gunten, U., 2007. Ag-doped carbon aerogels for removing halide ions in water treatment. *Water Res.* 41 (5), 1031–1037.

Shimizu, Y., Ateia, M., Yoshimura, C., 2018. Natural organic matter undergoes different molecular sieving by adsorption on activated carbon and carbon nanotubes. *Chemosphere* 203, 345–352.

Silver, S., 2003. Bacterial silver resistance: molecular biology and uses and misuses of silver compounds. *FEMS (Fed. Eur. Microbiol. Soc.) Microbiol. Rev.* 27 (2–3),

- 341–353.
- Song, H., Orr, O., Hong, Y., Karanfil, T., 2009. Isolation and fractionation of natural organic matter: evaluation of reverse osmosis performance and impact of fractionation parameters. *Environ. Monit. Assess.* 153 (1–4), 307.
- Strydom, C., van Staden, J., Strydom, H., 1990. An XPS investigation of silver chloride coated ion-selective electrodes. *J. Electroanal. Chem. Interfacial Electrochem.* 277 (1–2), 165–177.
- Strydom, C., van Staden, J., Strydom, H., 1991. An XPS investigation of the influence of bromide and iodide solutions on the surface of silver chloride coated ion-selective electrodes. *Electroanalysis* 3 (3), 197–201.
- Takaesu, H., Matsui, Y., Nishimura, Y., Matsushita, T., Shirasaki, N., 2019. Micromilling super-fine powdered activated carbon decreases adsorption capacity by introducing oxygen/hydrogen-containing functional groups on carbon surface from water. *Water Res.*
- Watson, K., Farré, M.J., Knight, N., 2012. Strategies for the removal of halides from drinking water sources, and their applicability in disinfection by-product minimisation: a critical review. *J. Environ. Manag.* 110, 276–298.
- Weinberg, H.S., Krasner, S.W., Richardson, S.D., Thruston Jr., A.D., 2002. The Occurrence of Disinfection By-Products (DBPs) of Health Concern in Drinking Water: Results of a Nationwide DBP Occurrence Study. National Exposure Research Laboratory, Athens, Ga.
- Zang, Y., Farnood, R., 2008. Photocatalytic activity of AgBr/TiO₂ in water under simulated sunlight irradiation. *Appl. Catal. B Environ.* 79 (4), 334–340.
- Zhang, H., Gao, X., Guo, T., Li, Q., Liu, H., Ye, X., Guo, M., Wu, Z., 2011. Adsorption of iodide ions on a calcium alginate–silver chloride composite adsorbent. *Colloid. Surf. Physicochem. Eng. Asp.* 386 (1–3), 166–171.